



Contents lists available at ScienceDirect

Journal of the Taiwan Institute of Chemical Engineers

journal homepage: www.elsevier.com/locate/jtice

Enhanced removal performance for methylene blue by kaolin with graphene oxide modification

Kai He^a, Guiqiu Chen^a, Guangming Zeng^{a,*}, Anwei Chen^{b,*}, Zhenzhen Huang^a, Jiangbo Shi^a, Min Peng^a, Tiantian Huang^a, Liang Hu^a

^a College of Environmental Science and Engineering, Hunan University and Key Laboratory of Environmental Biology and Pollution Control (Hunan University), Ministry of Education, Changsha 410082, PR China

^b College of Resources and Environment, Hunan Agricultural University, Changsha 410128, PR China

ARTICLE INFO

Article history:

Received 18 January 2018

Revised 1 April 2018

Accepted 12 April 2018

Available online 30 April 2018

Keywords:

Kaolin

Graphene oxide modification

Methylene blue

Adsorption process

ABSTRACT

In this study, graphene oxide modified kaolin (GO-kaolin) composites (named 2% GK, 5% GK, and 10% GK) were synthesized by a facile method. Characterization results indicated the successful modification of GO on kaolin surface. To understand the dye removal performance of kaolin with GO modification, batch adsorption experiments were carried out using methylene blue (MB) as a model dye pollutant in various experimental conditions. The adsorption results showed that the increase of GO content in modified kaolin composite could effectively enhance the removal of MB from aqueous solution in each experiment condition, which was attributed to the increase of special surface area and active adsorption sites. Kinetic analysis of MB adsorption by GO-kaolin samples was shown a better fitting to pseudo-second-order kinetic models. The adsorption isotherm data were better fitted to Langmuir isotherm models. The values of thermodynamics constants suggested that the adsorption reaction was endothermic in nature. Furthermore, adsorption process of MB on kaolin was changed after the introduction of GO. An excellent regeneration performance of 10% GK was observed via the regeneration experiment. The results show that kaolin modified with suitable GO content is a high-efficiency and reusable adsorbent in the removal of MB from wastewater.

© 2018 Taiwan Institute of Chemical Engineers. Published by Elsevier B.V. All rights reserved.

1. Introduction

With the rapid economic development, various types of pollutants including heavy metals [1,2], organic compounds [3–6], and dyes [7–10] will be inevitably or unconsciously released into environment, which will lead to severe environmental problems. Water resource is vital for the development and survival of human, however, water pollution caused by these pollutants has become a critical issue worldwide [11]. Among these pollutants, dyes, a kind of colored chemical agents, have been attracted great attentions due to their wide productions and applications [12]. Unfortunately, the discharge of dyes into water bodies is the major source of water pollution. Because of their undesirable diverse colors in waters even at low concentration (less than 1 ppm) and toxicity, they have been considered as a major threat to environment. Commonly, they will cause the abnormal coloration of surface waters, hinder the infiltration of sunlight and pose severe damage to the

aquatic organisms [13,14]. To date, dyes wastewater treatment is still a serious challenge to environmental scientists. Several commonly used treatment technologies including adsorption [15–19], membrane filtration [20], coagulation–flocculation [21], oxidation processes [22,23], and biodegradation [24,25] have been applied for dyes removal. However, each of these methods has their own benefits and limitations, which have been summarized in previous reviews [26–28].

Adsorption has been considered as an efficient and attractive method in pollutants removal due to its low-cost, high efficiency, and easy design [16]. Currently, various low-cost and eco-friendly adsorbents including natural inorganic and agricultural materials have been reported for the removal of dyes from aqueous solutions. Particularly, kaolin as one of the common clay mineral materials has been widely used in wastewaters treatment [29–31]. Due to its chemical composition and crystalline structure, the surfaces of kaolin are believed to carry a constant structural negative charge derived from the isomorphous substitution of Si(IV) by Al(III) in silica layer [32]. Therefore, it could be used as adsorbent for the treatment of cationic dyes wastewater [16,31–34]. However, the existing disadvantages such as severe agglomeration and low

* Corresponding authors.

E-mail addresses: zgming@hnu.edu.cn (G. Zeng), A.Chen@hunau.edu.cn (A. Chen).

adsorption capacity in solution will impede its practical applications [7,29]. Methylene blue (MB), a kind of phenothiazine salt, was selected as a model cationic dye in this study. In a preliminary experiment, we have verified the low adsorption performance of kaolin on MB. Likewise, it has been reported that the maximum adsorption capacity of MB by raw kaolin was only 13.99 mg/g [33]. Consequently, it is necessary to seek a simple and effective method to activate the adsorption capacity of kaolin.

Graphene oxide (GO), one of the typical graphene materials, has a unique two-dimensional (2D) atomic crystal with a single layer of sp²-bonded carbon atoms closely packed into honeycomb lattice [35,36]. It has become the research hotspot due to the intriguing structure and physicochemical properties [37,38]. In addition, GO has abundant oxygen containing functional groups and has been reported as good adsorbent for the removal of cationic dyes [39,40]. However, the separation of GO from aqueous solution is difficult due to its excellent hydrophilicity. Thus, the design of hybrid GO-based materials is important for pollutants removal. Previous studies have shown that GO enwrapped nanomaterial photocatalysts could enhance the adsorption, photocatalytic activity, and stability [41,42]. In a word, GO modification is an ideal route to improve the removal performance of other materials towards special pollutants. With this in mind, it is expected that hybridizing GO with kaolin may lead to considerable performance in dyes removal. To our knowledge, little research has been carried out to utilize the GO and kaolin composite for cationic dyes removal. Thus, the application of GO as an adsorption activator on kaolin for dyes wastewater treatment is worth exploring.

To take advantage of the recent developments in graphene and kaolin materials, a set of modified kaolin composites containing different contents of GO (GO-kaolin) using 3-aminopropyltrimethoxysilane (APTMS) as linkage were produced in laboratory through simple electrostatic interaction. In the present study, the main objectives were to investigate the adsorption processes and behaviors of MB on the as-prepared GO-kaolin composites from aqueous solution. Herein, we deem that this study can provide theoretical basis for further design and practical applications of graphene modified clay composites in future work.

2. Materials and methods

2.1. Materials

GO was prepared according to the modified Hummers method [43] and was confirmed before use in Supplementary Materials. APTMS, Kaolin (Al₂Si₂O₉H₄), MB, and all other chemicals used were purchased from Shanghai First Reagent Co., China. Solutions were prepared with distilled water in all experiments.

2.2. Synthesis of GO-kaolin nanocomposites

The synthesis of GO-kaolin was conducted by the electrostatic interaction using APTMS as linkage [44]. In this study, 1.0 g kaolin powder was first dispersed in 200 mL distilled water by magnetic stirring and ultrasonication for 2 h. Then, adding 4 mL APTMS into the suspension while stirring for 10 min, followed by adding different amounts of GO suspension to change the weight ratio of GO to kaolin (2%, 5%, and 10%) under vigorous stirring. After stirring for another 2 h, the composites were separated by filtration and washed with distilled water for three times. The composites were dried at 50 °C overnight to obtain the GO-kaolin samples. According to the GO content, the resultant GO-kaolin samples were named as 2% GK, 5% GK, and 10% GK, respectively. The preparation illustration of GO-kaolin is shown in Scheme S1.

2.3. Characterizations

The element compositions and surface functional groups of raw kaolin and GO-kaolin samples were investigated by X-ray photoelectron spectroscopy (XPS), which was performed on ESCALAB 250Xi (Thermo Fisher Scientific, USA). Field Emission Scanning Electron Microscope (FE-SEM, JSM-6700F, Japan) was used to observe the surface morphology of composites. The specific surface area was measured based on Brunauer–Emmett–Teller (BET) method using nitrogen as absorbent.

2.4. Adsorption experiments

In this study, the cationic dye, MB was used as the model pollutant to investigate the adsorption performance of GO-kaolin samples. Batch adsorption experiments were carried out at room temperature (25 ± 1 °C) by adding a known amount of adsorbent (80 mg) into 100 mL MB solution (pH 7.0) in a shaking bath with a shaking speed of 180 rpm. Initial dye concentrations (5–40 mg/L) were chosen to investigate the concentration effect. Herein, a set initial dye concentration of 20 mg/L was used for the following adsorption experiments in other solution conditions. Effect of solution pH ranged from 4.0 to 11.5 on the dye removal was examined. Different mass of adsorbents were employed to explore the effect of adsorbent dosage in a range of 0.4–1.6 g/L. The temperatures of solutions at the desired values (15 °C, 25 °C, 35 °C, and 45 °C) were controlled for the adsorption thermodynamics analysis. To study the effect of ionic strength on the dye adsorption, different concentrations of NaCl solutions (5–50 mM) were adjusted in the mixture. The dye concentration was measured at 664 nm by using a UV–vis spectrophotometer (UV-2550) based on a standard curve. The removal efficiency (*R*) and adsorption capacity (*Q_e* (mg/g)) of MB were determined with the following equations, respectively:

$$R = \frac{C_0 - C_e}{C_0} \times 100\% \quad (1)$$

$$Q_e = \frac{(C_0 - C_e)}{m} \times V \quad (2)$$

where *C₀* and *C_e* (mg/L) are the initial and equilibrium dye concentrations, respectively. *V* (L) represents the volume of dye solution, and *m* (g) is the mass of adsorbent added into the dye solution.

3. Results and discussion

3.1. Characterization of raw kaolin and GO-kaolin

The successful synthesis of GO was confirmed by characterization analysis. As can be seen from the SEM image (Fig. S1), the typical ripples are presented on GO surface [45]. Moreover, Fig. S2a and b showed the obvious characteristic peaks of oxygen-containing groups, D band and G band, respectively. For example, the vibration bands of O–H at 3394 cm⁻¹, the stretching vibration of the C=O group at 1726 cm⁻¹, the stretching vibration bands of O–C=O, C–O at 1400 cm⁻¹, 1055 cm⁻¹, respectively, indicating the successful preparation of GO [46]. In our experiment, GO-kaolin composites were prepared by binding GO flakes to kaolin with help of APTMS. The surface of kaolin will be positively charged after grafting with APTMS, thereby combining with negatively charged GO sheets by instant electrostatic interactions [44,47]. The color change of raw kaolin powder from white to brown after GO modification verified the successful introduction of GO sheets. This phenomenon is agreement with the observation of Zhang's group [44]. The morphological characteristics of kaolin and GO-kaolin samples were obtained by SEM (Fig. 1). The particle size of kaolin was rather inhomogeneous, and the small particles could form larger

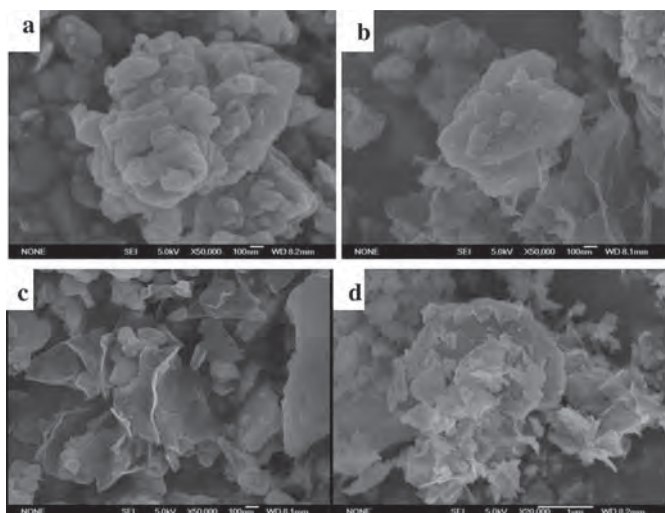


Fig. 1. SEM images of raw kaolin (a) and GO-kaolin samples: 2% GK (b); 5% GK (c), and 10% GK (d).

Table 1
Element composition, atom ratios, and BET- N_2 surface area (SA) of adsorbents.

Samples	Atom percentage (%)					SA (m ² /g)
	C1s	N1s	O1s	Si2p	Al2p	
Kaolin	8.55	0.55	58.68	17.38	14.84	9.65
2% GK	20.00	2.08	50.84	15.51	11.57	13.47
5% GK	22.18	1.86	50.26	14.52	11.18	19.06
10% GK	30.43	3.78	43.98	13.55	8.25	24.92

aggregates which distributed on the surface and periphery of large particles as shown in Fig. 1a [44]. After modification with GO, it could be observed clearly that the kaolin flakes were wrapped by GO sheets with typical ripples structure (Fig. 1b–d), indicating the successful preparation of GO-kaolin samples. In this study, a low specific surface area (SA) of used raw kaolin about 9.65 m²/g was measured. As seen from Table 1, after 2%, 5%, and 10% GO modification, the corresponding SA increased by 0.4, 0.98, and 1.58 times, respectively. Obviously, the introduction of GO could increase the SA of kaolin.

The evidence of the introduction of GO on kaolin was further determined via the chemical composition and main functional groups analysis with XPS measurements. Fig. 2a showed the XPS survey spectra of kaolin and GO-kaolin samples. The characteristic elements such as Al (80.72 eV), Si (108.7 eV), and O (540.7 eV) were found in the raw kaolin [7]. The detection of a little C and N was derived from the impurities. After GO modification using APTMS as linkage, a new element N at 409.63 eV was emerged in GO-kaolin samples. To better understand the changes after GO introduction, high-resolution scan of C1s spectra of 2% GK, 5% GK, and 10% GK samples were carried out. The spectra can be deconvoluted into three different peaks that correspond to carbon atoms in different functional groups. The peaks centered at the binding energies of about 284.6, 285.9, and 286.7 eV were observed (Fig. 2b), corresponding to C–C, C–N, and C–O [48]. The presence of C–N was attributed to the reaction of the introduced –NH₂ on the kaolin surface with the –COOH and C=O on the GO surface [44,47]. Furthermore, the element contents of kaolin and GO-kaolin based on XPS analysis are listed in Table 1. With the increase of GO content in the modified kaolin composites, the content of carbon atom increased from 8.55% to 30.43% and the content of oxygen atom decreased from 58.68% to 43.98%. The changes of elements ratio in kaolin samples indicated that the successful surface modification of kaolin with GO.

3.2. Adsorption studies

3.2.1. Effect of initial dye concentration

The variations in the removal efficiency of MB at different initial concentrations (5–40 mg/L) on four adsorbents are shown in Fig. 3. It can be observed from the figure that the adsorption trends of MB on the adsorbents showed similar decreasing trends with the increase of initial MB concentration. Because the increased competition for the active sites on the adsorbents at higher dye concentration solution will lead to the saturation of active sites, causing the decrease of adsorption efficiency [49,50]. In addition, the modification of GO on kaolin could obviously enhance the removal of dye. For example, at the same initial dye concentration of 20 mg/L, the adsorption affinities of dye to four adsorbents followed the order of kaolin < 2% GK < 5% GK < 10% GK. Compared with kaolin, dye removal of which was only 16.04%, whereas the dye removal efficiency increased by 0.91, 2.38, and 4.74 times by 2% GK (30.64%), 5% GK (54.23%), and 10% GK (92%), respectively. The increasing

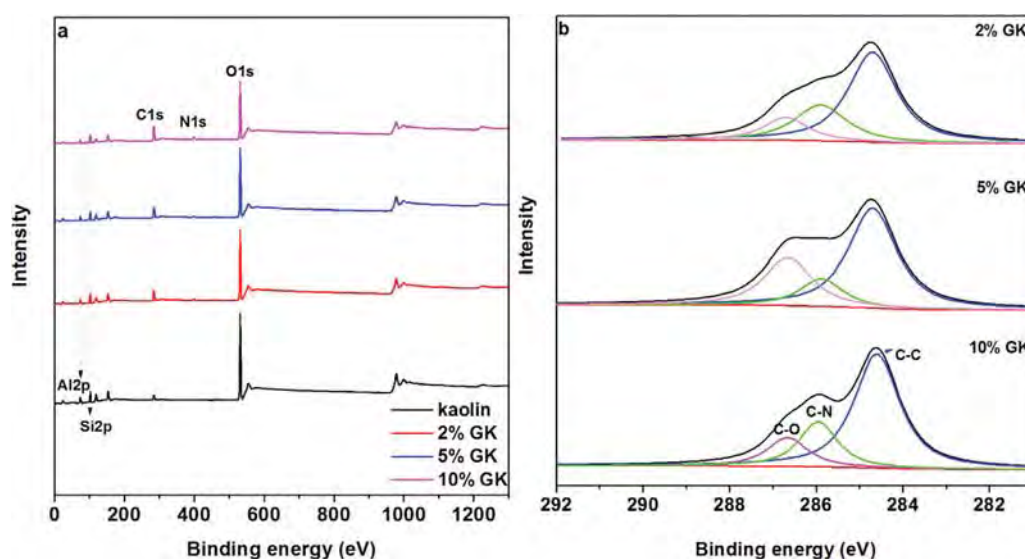


Fig. 2. XPS survey spectra of kaolin and GO-kaolin samples (a), and C1s XPS spectra of GO-kaolin samples (b).

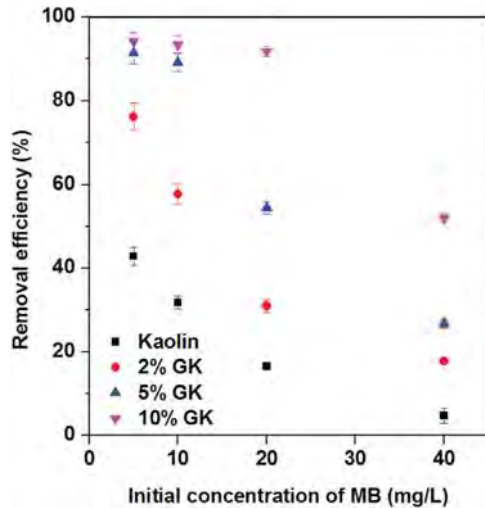


Fig. 3. Effect of initial concentration of MB on the adsorption by kaolin and GO-kaolin samples.

trend was correlated with the SA of kaolin samples (Table 1). However, the increased extent of SA was lower than the corresponding increased adsorption efficiency. Thus, the increase of adsorption was not merely attributed to the increase of SA, the π - π interactions between the π system of GO and the π unit of dye molecules also played an important role in the adsorption [51]. The results showed that the modification of kaolin with GO is a feasible approach to enhance the MB removal performance by kaolin.

3.2.2. Effect of adsorbent dosage

As shown in Fig. 4a, the removal efficiency of MB by four adsorbents showed similar upward trend with the increase of adsorbent dosage. Compared with the low dosage of adsorbent, high adsorbent dosage possessed greater surface area and could provide more chances to adsorb dye molecules, thus enhancing the dye removal from solution [52]. Apparently, the dye removal by 10% GK was more superior than other adsorbents. After the critical dosage (0.8 g/L) of 10% GK, the adsorption increasingly slowed down until reaching the maximum adsorption value. Herein, we selected 10% GK as a typical adsorbent to understand the variation in the removal rate of MB (20 mg/L) with time at different dosages. In addition, the increase of adsorbent dosage could increase the initial adsorption rate and decrease the equilibrium time (Fig. 4b).

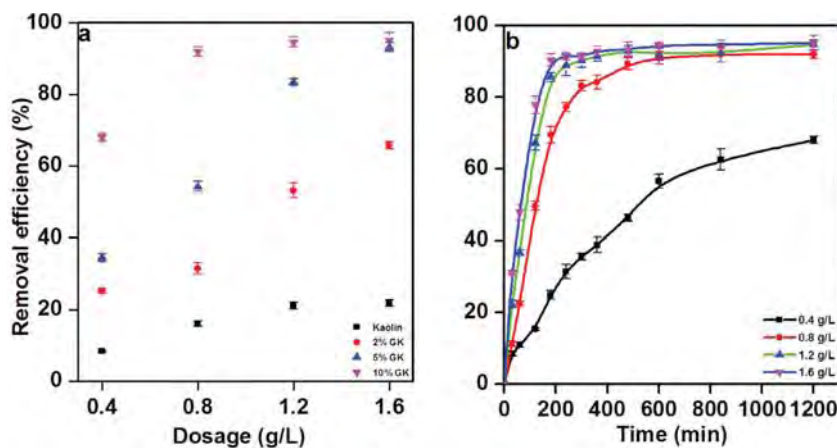


Fig. 4. Effect of adsorbents dosage on the adsorption of MB (a), and the effect of time and dosage of 10% GK on the MB removal (b).

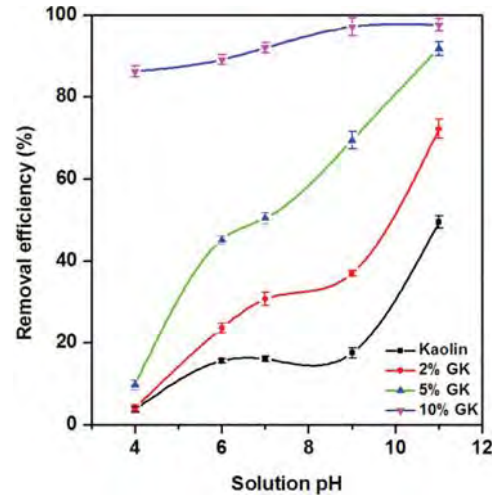


Fig. 5. Effect of solution pH on the removal of MB by adsorbents.

3.2.3. Effect of solution pH

The removal of MB by raw kaolin and GO modified kaolin was examined at the pH range from 4.0 to 11.5 as shown in Fig. 5. The increase of solution pH was beneficial to the removal of MB, as the removal efficiency of MB showed an increase trend [33]. The maximum removal values of MB by adsorbents were observed at pH 11.5. However, at low pH 4.0, the adsorbent of 10% GK can still remove large amount of MB (86.23%) from aqueous solution, whereas the removal efficiencies were lower than 10% by other adsorbents. This may be responsible for the high content of GO in the surface of kaolin that could provide more active sites and stronger adsorption interaction (π - π interactions) even at low pH.

3.2.4. Effect of ionic strength

The solution ionic strength is also one of the most important parameters that may influence the removal of pollutants [16]. Therefore, the effects of solution ionic strength on the removal of MB by four adsorbents were conducted. As shown in Fig. 6, although the removal of MB by kaolin and GO-kaolin changed little, the adsorption of MB on kaolin and 10% GK showed opposite trends with the increase of ionic strength. Generally, the screening of the surface charges caused by the presence of salts solution may decrease the adsorption; however, the salts solution also can enhance the adsorption of dye through reducing the degree of dissociation of the dye molecules [16,31]. Thus, the decrease of removal efficiency on MB by 10% kaolin indicated that the screening

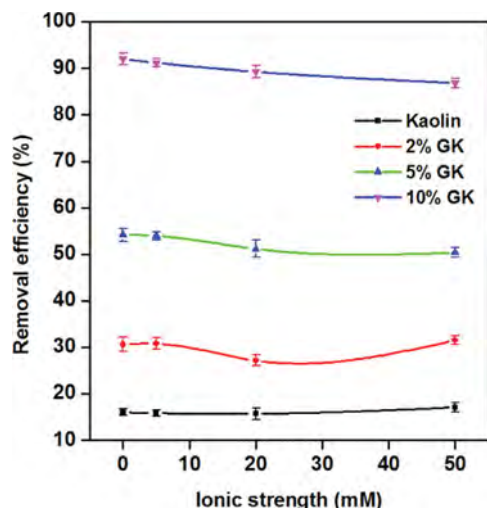


Fig. 6. Effect of ionic strength on the removal of MB by kaolin and GO-kaolin samples.

of the surface charges played main role in the adsorption behavior. In contrast, the later effect seemed to be dominant in the adsorption by kaolin [16].

3.2.5. Effect of temperature

The temperature is a significant parameter for the adsorption process. Fig. 7 showed the effect of temperature on the removal of MB by kaolin and GO-kaolin samples. Obviously, the removal of MB by kaolin and GO-kaolin samples was more favorable at higher temperature. The increase of temperature can enhance the movability of MB molecules, thus increasing the interaction chance between the adsorption actives sites and MB molecules.

The thermodynamic parameters change in Gibb's free energy (ΔG^0), entropy (ΔS^0) and enthalpy (ΔH^0) for the removal of MB by kaolin and GO-kaolin samples are determined from the equations as follow [16]:

$$\ln K_d = \frac{\Delta S^0}{R} - \frac{\Delta H^0}{RT} \quad (3)$$

$$\Delta G^0 = \Delta H^0 - T\Delta S^0 \quad (4)$$

where K_d is calculated from Q_e/C_e . T is absolute temperature in Kelvin (K), and R is the universal gas constant (8.314 kJ/(molK)).

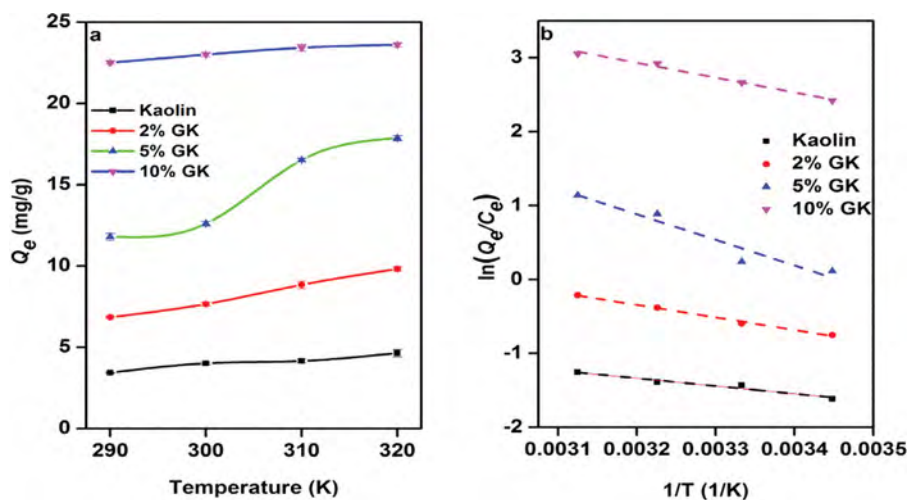


Fig. 7. Effect of temperature on the adsorption of MB by kaolin and GO-kaolin samples: adsorption capacity at different temperatures (a) and thermodynamic analysis (b).

Table 2
Thermodynamic parameters for the adsorption of MB onto kaolin and GO-kaolin samples.

Samples	Temperature (K)	ΔG^0 (kJ/mol)	ΔH^0 (kJ/mol)	ΔS^0 (J/(K mol))
	288	3.885	8.73	16.82
Kaolin	298	3.717		
	308	3.548		
	318	3.380		
	288	1.935		
2% GK	298	1.512		
	308	1.089	14.12	42.31
	318	0.665		
	288	0.141		
5% GK	298	-0.852		
	308	-1.846	28.76	99.37
	318	-2.840		
	288	-5.764		
10% GK	298	-6.544		
	308	-7.324	16.70	78.00
	318	-8.104		

ΔH^0 and ΔS^0 are determined from the slope and intercept of the Van't Hoff plots of $\ln K_d$ versus of $1/T$, respectively.

Table 2 listed the values of above thermodynamic parameters. It can be noticed that the values of ΔG^0 decreased with the increase of temperature. However, the values of ΔG^0 were positive at the kaolin and 2% GK treatments, indicating the adsorption of MB onto kaolin and 2% GK was a non-spontaneous process. In contrast, the negative values of ΔG^0 (5% GK (except 288 K) and 10% GK) suggested a spontaneous adsorption process [7]. The differences suggested that the modification of enough GO content onto kaolin should change the adsorption process. Meanwhile, the decrease of ΔG^0 values with the increase of temperature indicated that the adsorption of MB onto kaolin and GO-kaolin samples was more favorable at higher temperature. The positive values of ΔH^0 were the indication of the typical endothermic nature of adsorption reaction. Besides, the positive values of ΔS^0 implied that the degrees of randomness at the solid-solution interface increased during the adsorption [49]. All these thermodynamics parameters above-mentioned indicated that the modification with GO conducted to enhance the adsorption performance of raw kaolin.

3.3. Adsorption kinetics

In our study, the effects of time on the adsorption capacity of GO-kaolin samples were investigated. As shown in Fig. 8, the

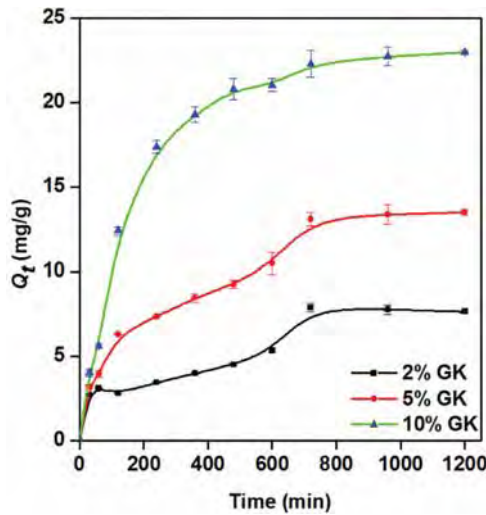


Fig. 8. The adsorption capacity of MB by GO-kaolin samples at different time.

adsorption rate was relatively rapid at initial stage, and then became more gradual until reaching the equilibrium. Obviously, both the adsorption rate and adsorption capacity of MB by 10% GK were higher than that of 2% GK and 5% GK at the same time condition, owing to the larger SA and more active sites of 10% GK. To understand the controlling mechanism of dye adsorption by adsorbents from aqueous solution, the experimental data were fitted with two commonly used kinetic models (pseudo-first-order and pseudo-second-order) [16,53].

3.3.1. Pseudo-first-order kinetic model

Pseudo-first-order equation is described as follows:

$$\ln(Q_e - Q_t) = \ln Q_e - k_1 t \quad (5)$$

where Q_t (mg/g) and Q_e (mg/g) are the amount of adsorbed dye molecules on the adsorbent at different contact time (t) and equilibrium time, respectively. k_1 (min^{-1}) is the pseudo-first-order rate constant. The fitted curve is shown in Fig. 9a.

3.3.2. Pseudo-second-order kinetic model

Pseudo-second-order equation is described as follows:

$$\frac{t}{Q_t} = \frac{1}{k_2 Q_e^2} + \frac{t}{Q_e} \quad (6)$$

where k_2 ($\text{g}/\text{mg min}$) is the pseudo-second-order rate constant. The fitted curve is displayed in Fig. 9b.

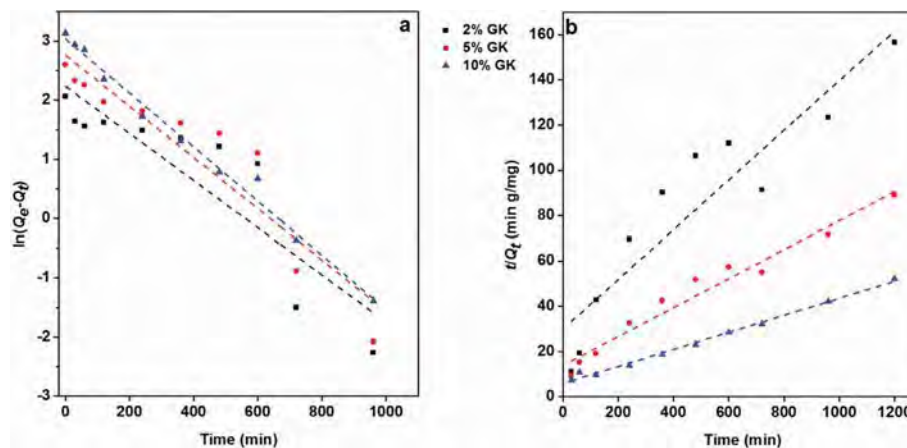


Fig. 9. Pseudo-first-order kinetics model (a) and pseudo-second kinetics model (b) for the adsorption of MB on GO-kaolin samples.

The calculated kinetic parameters of two models are given in Table 3. It can be clearly observed from the table that pseudo-second-order kinetic model for each GO-kaolin sample showed a better correlation coefficient in comparison with the pseudo-first-order kinetic model, indicating that pseudo-second-order model was a better model for describing the kinetic of GO-kaolin toward MB. Generally, the pseudo-second-order kinetic model is based on the assumption that chemisorption is the rate-limiting step [32,54]. Thus, it could be inferred that the adsorption process of MB on GO-kaolin samples was chemisorption.

3.4. Adsorption equilibrium

The adsorption capacity of MB by GO-kaolin samples corresponding to the equilibrium concentration in aqueous solution is presented in Fig. 10. Two most common types of isotherms, Langmuir and Freundlich isotherm models were employed to explain the interaction of adsorbate molecules and adsorbent surface. The curves of the two fitted isotherm models are shown in Fig. 10.

3.4.1. Freundlich isotherm

The Freundlich isotherm model is an exponential equation that applied to describe the adsorption behavior on the heterogeneous surface [32]. The well-known expression for Freundlich isotherm model is shown as following non-linear equation:

$$Q_e = K_F C_e^{1/n} \quad (7)$$

where Q_e (mg/g) is the equilibrium adsorption capacity of GO-kaolin towards MB, C_e (mg/L) is the concentration of MB at adsorption equilibrium. K_F [$(\text{mg/g})(\text{L/mg})^{1/n}$] is the adsorption equilibrium constant of Freundlich isotherm model. n is the Freundlich constant giving an indication of how favorable the adsorption process. When $0 < 1/n < 1$, the adsorption is favorable; when the value of $1/n$ beyond 1, the adsorption is unfavorable; when $1/n = 1$, indicating the adsorption is homogeneous [55].

3.4.2. Langmuir isotherm

The Langmuir isotherm is based on the assumption that the adsorption active sites distribute homogeneously over the surface of adsorbent. These active sites have the same affinity for adsorption of a single molecular layer and there is no interaction between adsorbed molecules [32]. The equation of Langmuir isotherm is represented as below:

$$Q_e = \frac{Q_m K_L C_e}{1 + K_L C_e} \quad (8)$$

where Q_m (mg/g) is the theoretical maximum adsorption capacity of adsorbent, and K_L (L/mg) is Langmuir isotherm constant.

Table 3
Kinetic parameters for the adsorption of MB onto GO-kaolin samples.

Models	Pseudo-first-order			Pseudo-second-order		
	$Q_{e(cal)}$ (mg/g)	k_1 (min^{-1})	R^2	$Q_{e(cal)}$ (mg/g)	k_2 (g/mg min)	R^2
2% GK	9.33	0.0040	0.767	9.11	0.0004	0.845
5% GK	15.85	0.0043	0.857	15.65	0.0003	0.960
10% GK	20.81	0.0046	0.986	26.52	0.0002	0.993

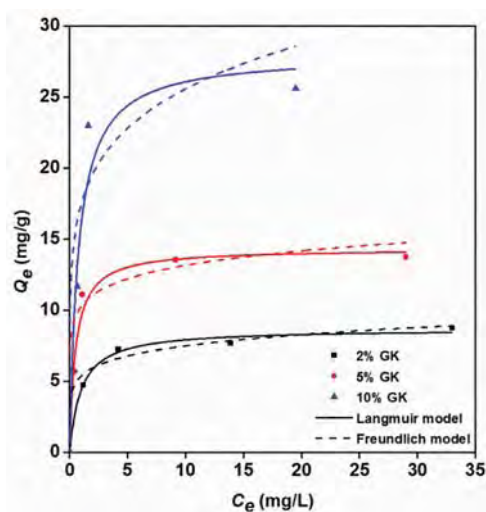


Fig. 10. The adsorption isotherms of MB by GO-kaolin samples; the data from experiment have been fitted by Langmuir and Freundlich isotherm models.

Table 4 showed the calculated values of Freundlich and Langmuir models' parameters. It can be found from the correlation coefficient (R^2) of each GO-kaolin sample that Langmuir isotherm models were better fitted the experiment data than Freundlich isotherm models. Furthermore, it showed that the Q_m of 10% GK (28.016 mg/g) for MB was approximately 1.95 times and 3.22 times that of 5% GK (14.335 mg/g) and 2% GK (8.696), respectively. Compared with other reported adsorbent materials (Table 5), 10% GK showed satisfactory removal performance for MB. Thus, the modification on kaolin with a certain content of GO could enhance the adsorption capacity on MB at various concentrations.

3.5. Desorption and regeneration evaluation

The regeneration capacity of adsorbent is an important factor to evaluate the availability in the practical application [57]. In this study, desorption experiment was conducted using 10% GK as model adsorbent due to its high removal efficiency towards MB. The desorption of MB from 10% GK was performed at acidic ethanol solution. Similar to previous reports, with increasing regeneration cycles, the dye removal by 10% GK decreased, which was attributed to the increased dye molecules that attached to adsorbent surface via chemisorption [7,49]. After five cycles, the removal efficiency of MB by the regenerated 10% GK can still remain

Table 5
Maximum adsorption capacity (Q_m , mg/g) of MB by various adsorbents in other reports.

Adsorbents	Q_m (mg/g)	References
Raw kaolin	13.99	[33]
Graphene oxide	193.902	[40]
Magnetic multi-wall carbon nanotube	15.87	[17]
Zeolite	22	[52]
Coir pith carbon	5.87	[56]
10% GK	28.016	In this study

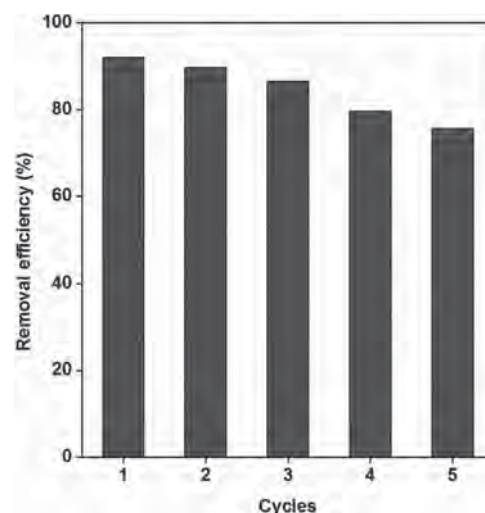


Fig. 11. Adsorption of MB on GO-kaolin (10% GK) in five cycles.

at about 75.6%, which was still higher than that by raw kaolin (Fig. 11). Thus, the application of suitable GO-kaolin is recyclable and will reduce the overall cost for the adsorbent.

4. Conclusions

In this study, the GO modified kaolin composites were successfully prepared by a facile method and used to investigate the removal performance of MB dye from aqueous solutions. Obviously, the increase of GO content on kaolin enhanced the adsorption of MB, owing to the increasing surface area and adsorption active sites. The kinetic analysis based on the experiment data suggested that the adsorption can be better described by a pseudo-second-order kinetics model. Langmuir isotherm model was found to better describe the adsorption behavior according to the data fitting.

Table 4
The parameters of adsorption isotherms for MB onto GO-kaolin samples.

Isotherms	Freundlich			Langmuir		
	K_f [(mg/g)(L/mg) $^{1/n}$]	$1/n$	R^2	Q_m (mg/g)	K_L (L/mg)	R^2
2% GK	5.380	0.1444	0.821	8.696	1.0225	0.939
5% GK	10.298	0.1068	0.757	14.335	1.9877	0.896
10% GK	17.497	0.1652	0.847	28.016	1.3516	0.869

Furthermore, the MB removal was favorable at higher temperature and higher solution pH. Besides, the adsorption process of kaolin and 2% GK for MB were non-spontaneous, whereas the adsorption of MB by 10% GK followed a spontaneous process. Findings of this work can provide a basis for further designing novel graphene modified clay materials for various environmental applications.

Acknowledgments

This study was financially supported by the National Natural Science Foundation of China (51579099, 51521006 and 51508186), the Program for Changjiang Scholars and Innovative Research Team in University (IRT-13R17), the Hunan Provincial Natural Science Foundation of China (2016JJ3076), and the Hunan Provincial Innovation Foundation for Postgraduate (CX2016B134).

Supplementary materials

Supplementary material associated with this article can be found, in the online version, at doi:10.1016/j.jtice.2018.04.013.

References

- Liang J, Yang Z, Tang L, Zeng G, Yu M, Li X, et al. Changes in heavy metal mobility and availability from contaminated wetland soil remediated with combined biochar-compost. *Chemosphere* 2017;181:281–8.
- Wu H, Lai C, Zeng G, Liang J, Chen J, Xu J, et al. The interactions of composting and biochar and their implications for soil amendment and pollution remediation: a review. *Crit Rev Biotechnol* 2017;37:754.
- Cheng M, Zeng G, Huang D, Cui L, Xu P, Zhang C, et al. Hydroxyl radicals based advanced oxidation processes (AOPs) for remediation of soils contaminated with organic compounds: A review. *Chem Eng J* 2016;284:582–98.
- Yang C, Chen H, Zeng G, Yu G, Luo S. Biomass accumulation and control strategies in gas biofiltration. *Biotechnol Adv* 2010;28:531–40.
- Cheng Y, He H, Yang C, Zeng G, Li X, Chen H, et al. Challenges and solutions for biofiltration of hydrophobic volatile organic compounds. *Biotechnol Adv* 2016;34:1091–102.
- Chen M, Xu P, Zeng G, Yang C, Huang D, Zhang J. Bioremediation of soils contaminated with polycyclic aromatic hydrocarbons, petroleum, pesticides, chlorophenols and heavy metals by composting: Applications, microbes and future research needs. *Biotechnol Adv* 2015;33:745–55.
- Huang Q, Liu M, Chen J, Wang K, Xu D, Deng F, et al. Enhanced removal capability of kaolin toward methylene blue by mussel-inspired functionalization. *J Mater Sci* 2016;51:8116–30.
- Raghu S, Ahmed BC. Chemical or electrochemical techniques, followed by ion exchange, for recycle of textile dye wastewater. *J Hazard Mater* 2007;149:324–30.
- Neelavannan MG, Revathi M, Basha CA. Photocatalytic and electrochemical combined treatment of textile wash water. *J Hazard Mater* 2007;149:371–8.
- Xian Y, Wu Y, Guo X, Lu Y, Luo H, Luo D, et al. Simultaneous determination of 11 restricted dyes in cosmetics by ultra high-performance liquid chromatography/tandem mass spectrometry. *Anal Methods* 2013;5:1965–74.
- Tang WW, Zeng GM, Gong JL, Liang J, Xu P, Zhang C, et al. Impact of humic/fulvic acid on the removal of heavy metals from aqueous solutions using nanomaterials: A review. *Sci Total Environ* 2014;468–469:1014–27.
- Robinson T, McMullan G, Marchant R, Nigam P. Remediation of dyes in textile effluent: A critical review on current treatment technologies with a proposed alternative. *Bioresour Technol* 2001;77:247–55.
- Khan R, Bhawana P, Fulekar MH. Microbial decolorization and degradation of synthetic dyes: A review. *Rev Environ Sci Biotechnol* 2013;12:75–97.
- Cheung WH, Szeto YS, McKay G. Enhancing the adsorption capacities of acid dyes by chitosan nano particles. *Bioresour Technol* 2009;100:1143–8.
- Gil A, Assis FCC, Albeniz S, Korili SA. Removal of dyes from wastewaters by adsorption on pillared clays. *Chem Eng J* 2011;168:1032–40.
- Tehrani-Bagha AR, Nikkar H, Mahmoodi NM, Markazi M, Menger FM. The sorption of cationic dyes onto kaolin: Kinetic, isotherm and thermodynamic studies. *Desalination* 2011;266:274–80.
- Gong JL, Wang B, Zeng GM, Yang CP, Niu CG, Niu QY, et al. Removal of cationic dyes from aqueous solution using magnetic multi-wall carbon nanotube nanocomposite as adsorbent. *J Hazard Mater* 2009;164:1517–22.
- Tan X, Liu Y, Zeng G, Wang X, Hu X, Gu Y, et al. Application of biochar for the removal of pollutants from aqueous solutions. *Chemosphere* 2015;125:70–85.
- Deng J, Zhang X, Zeng G, Gong J, Niu Q, Liang J. Simultaneous removal of Cd (II) and ionic dyes from aqueous solution using magnetic graphene oxide nanocomposite as an adsorbent. *Chem Eng J* 2013;226:189–200.
- Shi C, Lv C, Wu L, Hou X. Porous chitosan/hydroxyapatite composite membrane for dyes static and dynamic removal from aqueous solution. *J Hazard Mater* 2017;338:241–9.
- Moghaddam SS, Moghaddam MRA, Arami M. Coagulation/flocculation process for dye removal using sludge from water treatment plant: optimization through response surface methodology. *J Hazard Mater* 2010;175:651–7.
- Wang H, Yuan X, Wu Y, Zeng G, Chen X, Leng L, et al. Synthesis and applications of novel graphitic carbon nitride/metal-organic frameworks mesoporous photocatalyst for dyes removal. *Appl Catal B: Environ* 2015;174:445–54.
- Xu P, Zeng GM, Huang DL, Feng CL, Hu S, Zhao MH, et al. Use of iron oxide nanomaterials in wastewater treatment: A review. *Sci Total Environ* 2012;424:1–10.
- Zeng G, Cheng M, Huang D, Lai C, Xu P, Wei Z, et al. Study of the degradation of methylene blue by semi-solid-state fermentation of agricultural residues with *Phanerochaete chrysosporium* and reutilization of fermented residues. *Waste Manag* 2015;38:424–30.
- He K, Chen G, Zeng G, Huang Z, Guo Z, Huang T, et al. Applications of white rot fungi in bioremediation with nanoparticles and biosynthesis of metallic nanoparticles. *Appl Microbiol Biotechnol* 2017;12:4853–62.
- Crini G. Non-conventional low-cost adsorbents for dye removal: a review. *Bioresour Technol* 2006;97:1061–85.
- Robinson T, McMullan G, Marchant R, Nigam P. Remediation of dyes in textile effluent: A critical review on current treatment technologies with a proposed alternative. *Bioresour Technol* 2001;77:247–55.
- Forgacs E, Cserháti T, Oros G. Removal of synthetic dyes from wastewaters: A review. *Environ Int* 2004;30:953–71.
- Huang Q, Liu M, Deng F, Wang K, Huang H, Xu D, et al. Mussel inspired preparation of amine-functionalized kaolin for effective removal of heavy metal ions. *Mater Chem Phys* 2016;181:116–25.
- Arias M, Barral MT, Mejuto JC. Enhancement of copper and cadmium adsorption on kaolin by the presence of humic acids. *Chemosphere* 2002;48:1081–8.
- Nandi BK, Goswami A, Purkait MK. Removal of cationic dyes from aqueous solutions by kaolin: kinetic and equilibrium studies. *Appl Clay Sci* 2009;42:583–90.
- Nandi BK, Goswami A, Purkait MK. Adsorption characteristics of brilliant green dye on kaolin. *J Hazard Mater* 2009;161:387–95.
- Ghosh D, Bhattacharyya KG. Adsorption of methylene blue on kaolinite. *Appl Clay Sci* 2002;20:295–300.
- Harris RG, Wells JD, Angove MJ, Johnson BB. Modeling the adsorption of organic dye molecules to kaolinite. *Clays Clay Miner* 2006;54:456–65.
- Novoselov KS, Fal'ko VI, Colombo L, Gellert PR, Schwab MG, Kim K. A roadmap for graphene. *Nature* 2012;490:192–200.
- He K, Chen G, Zeng G, Peng M, Huang Z, Shi J, et al. Stability, transport and ecosystem effects of graphene in water and soil environments. *Nanoscale* 2017;9:5370–88.
- Wang H, Yuan X, Wu Y, Huang H, Peng X, Zeng G, et al. Graphene-based materials: fabrication, characterization and application for the decontamination of wastewater and wastegas and hydrogen storage/generation. *Adv Colloid Interface Sci* 2013;195–196:19–40.
- Zhang Y, Zeng GM, Tang L, Chen J, Zhu Y, He XX, et al. Electrochemical sensor based on electrodeposited graphene-Au modified electrode and nanoAu carrier amplified signal strategy for attomolar mercury detection. *Anal Chem* 2015;87:989–96.
- Ramesha GK, Vijaya Kumara A, Muralidhara HB, Sampath S. Graphene and graphene oxide as effective adsorbents toward anionic and cationic dyes. *J Colloid Interface Sci* 2011;361:270–7.
- Zhang W, Zhou C, Zhou W, Lei A, Zhang Q, Wan Q, et al. Fast and considerable adsorption of methylene blue dye onto graphene oxide. *Bull Environ Contam Toxicol* 2011;87:86–90.
- Zhu M, Chen P, Liu M. Graphene oxide enwrapped Ag/AgX (X= Br, Cl) nanocomposite as a highly efficient visible-light plasmonic photocatalyst. *ACS Nano* 2011;5:4529–36.
- Liu L, Liu J, Sun DD. Graphene oxide enwrapped Ag₃PO₄ composite: towards a highly efficient and stable visible-light-induced photocatalyst for water purification. *Catal Sci Technol* 2012;2:2525–32.
- Sun L, Yu H, Fugetsu B. Graphene oxide adsorption enhanced by in situ reduction with sodium hydrosulfite to remove acridine orange from aqueous solution. *J Hazard Mater* 2012;203–204:101–10.
- Zhang R, Alecrim V, Hummelgård M, Andres B, Forsberg S, Andersson M, et al. Thermally reduced kaolin-graphene oxide nanocomposites for gas sensing. *Sci Rep* 2015;5:7676.
- Wang J, Chen Z, Chen B. Adsorption of polycyclic aromatic hydrocarbons by graphene and graphene oxide nanosheets. *Environ Sci Technol* 2014;48(9):4817–25.
- Wang J, Chen B. Adsorption and coadsorption of organic pollutants and a heavy metal by graphene oxide and reduced graphene materials. *Chem Eng J* 2015;281:379–88.
- Yoon T, Kim J, Kim J, Lee JK. Electrostatic self-assembly of Fe₃O₄ nanoparticles on graphene oxides for high capacity lithium-ion battery anodes. *Energies* 2013;6:4830–40.
- Mao S, Yu K, Cui S, Bo Z, Lu G, Chen J. A new reducing agent to prepare single-layer, high-quality reduced graphene oxide for device applications. *Nanoscale* 2011;3:2849.
- Autam M, Hameed BH. Chitosan-clay composite as highly effective and low-cost adsorbent for batch and fixed-bed adsorption of methylene blue. *Chem Eng J* 2014;237:352–61.
- Huang Z, Chen G, Zeng G, Chen A, Zuo Y, Guo Z, et al. Polyvinyl alcohol-immobilized *Phanerochaete chrysosporium* and its application in the bioremediation of composite-polluted wastewater. *J Hazard Mater* 2015;289:174–83.

- [51] Wang J, Chen B. Adsorption and coadsorption of organic pollutants and a heavy metal by graphene oxide and reduced graphene materials. *Chem Eng J* 2015;281:379–88.
- [52] Rida K, Bouraoui S, Hadnine S. Adsorption of methylene blue from aqueous solution by kaolin and zeolite. *Appl Clay Sci* 2013;83–84:99–105.
- [53] Long F, Gong JL, Zeng GM, Chen L, Wang XY, Deng JH, et al. Removal of phosphate from aqueous solution by magnetic Fe–Zr binary oxide. *Chem Eng J* 2011;171:448–55.
- [54] Xu P, Zeng GM, Huang DL, Lai C, Zhao MH, Wei Z, et al. Adsorption of Pb(II) by iron oxide nanoparticles immobilized *Phanerochaete chrysosporium* : Equilibrium, kinetic, thermodynamic and mechanisms analysis. *Chem Eng J* 2012;203:423–31.
- [55] Rauf MA, Bukallah SB, Hamour FA, Nasir AS. Adsorption of dyes from aqueous solutions onto sand and their kinetic behavior. *Chem Eng J* 2008;137:238–43.
- [56] Kavitha D, Namasivayam C. Experimental and kinetic studies on methylene blue adsorption by coir pith carbon. *Bioresour Technol* 2007;98:14–21.
- [57] Zhang C, Lai C, Zen G, Huang D, Yang C, Wang Y, et al. Efficacy of carbonaceous nanocomposites for sorbing ionizable antibiotic sulfamethazine from aqueous solution. *Water Res* 2016;95:103–12.